



ARTICLE

An IgD-Fc-Ig fusion protein restrains the activation of T and B cells by inhibiting IgD-IgDR-Lck signaling in rheumatoid arthritis

Xiao-xi Hu¹, Ai-jun Zhang¹, Wen-wen Pan¹, Qian-ling Xin¹, Jing-yu Chen¹, Ling-ling Zhang¹, Yan Chang¹, Yu-jing Wu¹ and Wei Wei¹

Rheumatoid arthritis (RA) is a chronic systemic autoimmune disease characterized by synovitis and the destruction of small joints. Emerging evidence shows that immunoglobulin D (IgD) stimulation induces T-cell activation, which may contribute to diseases pathogenesis in RA. In this study, we investigated the downstream signaling pathways by which IgD activated T cells as well as the possible role of IgD in the T–B interaction. Peripheral blood mononuclear cells were isolated from peripheral blood of healthy controls and RA patients. We demonstrated that IgD activated T cells through IgD receptor (IgDR)-lymphocyte-specific protein tyrosine kinase (Lck)-zeta-associated protein 70 (ZAP70)/phosphatidylinositol 3-kinase (PI3K)/nuclear factor kappa-B (NF-κB) signaling pathways; IgD-induced CD4⁺ T cells promoted the proliferation of CD19⁺ B cells in RA patients. A novel fusion protein IgD-Fc-Ig (composed of human IgD-Fc domain and IgG₁ Fc domain, which specifically blocked the IgD–IgDR binding) inhibited the coexpression of IgDR and phosphorylated Lck (p-Lck) and the expression levels of p-Lck, p-ZAP70, p-PI3K on CD4⁺ T cells, and decreased NF-κB nuclear translocation in Jurkat cells. Meanwhile, IgD-Fc-Ig downregulated the expression levels of CD40L on CD4⁺ T cells as well as CD40, CD86 on CD19⁺ B cells in RA patients and healthy controls. It also decreased the expression levels of CD40L on CD4⁺ T cells and CD40 on CD19⁺ B cells from spleens of collagen-induced arthritis (CIA) mice and reduced IL-17A level in mouse serum. Moreover, administration of IgD-Fc-Ig (1.625–13 mg/kg, iv, twice a week for 4 weeks) in CIA mice dose-dependently decreased the protein expression levels of CD40, CD40L, and IgD in spleens. IgD-Fc-Ig restrains T-cell activation through inhibiting IgD-IgDR-Lck-ZAP70-PI3K-NF-κB signaling, thus inhibiting B-cell activation. Our data provide experimental evidences for application of IgD-Fc-Ig as a highly selective T cell-targeting treatment for RA.

Keywords: rheumatoid arthritis; immunoglobulin D; IgD-Fc-Ig; immunoglobulin D receptor; CD4⁺ T cells; CD19⁺ B cells

Acta Pharmacologica Sinica (2022) 43:387–400; <https://doi.org/10.1038/s41401-021-00665-w>

INTRODUCTION

Rheumatoid arthritis (RA) is an autoimmune disease characterized by persistent inflammation of synovial joints, bone destruction, loss of cartilage and increased risk of cardiovascular and other intercurrent diseases [1]. The treatment strategy currently in use mainly includes nonsteroidal anti-inflammatory drugs, conventional synthetic disease-modifying antirheumatic drugs, biological DMARDs, and targeted synthetic DMARDs [2]. However, some drugs are not suitable in some patients with contraindications or early intolerance during clinical use or are accompanied by serious adverse drug reactions, including severe bone marrow suppression, infection, and even tumors. Therefore, ~20%–30% of patients remain refractory to current therapies [3]. For these patients, new treatment options and better insights into the pathogenesis of RA are needed.

Immunoglobulin D (IgD) acts as a B-cell surface receptor in the form of membrane-bound IgD or in small amounts as secreted IgD (sIgD) in humans and mice [4]. IgD is an important immunomodulatory molecule and promotes immune defense by inducing the activation and infiltration of IgD-interacting cells into tissues and

their production of immune-activating factors, and overactivation of this pathway can cause inflammation and tissue damage [5, 6]. The regulation and functions of IgD remain poorly understood [7]. It has been reported that sIgD is abnormally highly expressed in the serum of patients with multiple diseases, such as immunodeficiency, chronic infection, and autoimmune disease [8]. In addition, our group further found abnormally sIgD in peripheral blood from RA patients and collagen-induced arthritis (CIA) mice. An association between detectable sIgD and biomarkers, including disease activity score in 28 joints, sRANKL, rheumatoid factor, C-reactive protein, and anti-cyclic citrullinated peptide, in patients with RA was observed [9, 10]. We further demonstrated that IgD could enhance activated T- and B-cell subsets in RA peripheral blood mononuclear cells (PBMCs) [10]. IgD exerts biological functions by binding to a specific membrane receptor (FcδR or IgD receptor (IgDR)) with high affinity [11]. Moreover, the N-linked glycans present in both the first and third constant regions of the δ heavy-chain domain are prerequisites for the binding of IgD to IgDR. Therefore, the CH₁–CH₃ domains are critical for the binding of IgD to IgDR and for the associated function [12]. In vivo and

¹Institute of Clinical Pharmacology, Anhui Medical University, Key Laboratory of Anti-inflammatory and Immune Medicine, Ministry of Education, Anhui Collaborative Innovation Center of Anti-inflammatory and Immune Medicine, Hefei 230032, China
Correspondence: Yu-jing Wu (wyj@ahmu.edu.cn) or Wei Wei (www@ahmu.edu.cn)

Received: 25 October 2020 Accepted: 19 March 2021

Published online: 16 April 2021

in vitro studies have suggested that IgDR on T cells might play a critical role in the regulation of IgD. Recently, we reported that IgD could regulate CD4⁺ T-cell activation accompanied by lymphocyte-specific protein tyrosine kinase (Lck) phosphorylation in RA patients and healthy controls [9]. Our group successfully synthesized a fusion protein known as IgD-Fc-Ig by connecting human IgD-Fc and IgG-Fc domains to specifically block IgD-IgDR crosslinking. IgD-Fc-Ig was observed to alleviate arthritis manifestations in CIA rodent models in vivo [9, 13].

It is unclear whether IgD activates downstream signaling pathways (Lck-zeta-associated protein 70 (ZAP70)-phosphatidylinositol 3-kinase (PI3K)-nuclear factor kappa-B (NF- κ B)) and activates T cells through the molecular interaction between IgDR and Lck, and the possible role of IgD in the T-B interaction remains unknown. Therefore, in this study, we performed in vitro and in vivo studies and determined that IgDR-Lck is critical in the molecular mechanisms of T-cell and B-cell activation stimulated by IgD. IgD-Fc-Ig plays a role in the regulation of IgD-activated T cells, providing evidence that targeting IgDR itself offers a feasible and effective therapeutic strategy for a large proportion of RA patients.

MATERIALS AND METHODS

Drugs and reagents

The IgD-Fc-Ig fusion protein and IgG₁-Fc protein were supplied by the Institute of Clinical Pharmacology, Anhui Medical University (Hefei, China), and IgD-Fc-Ig had a purity of more than 90% [13]. The Lck inhibitor A770041 was purchased from MedChemExpress (Cat. No. HY-11011, NJ, USA). The rhTNFR:Fc fusion protein was purchased from Guojian Pharmaceutical Company (Shanghai, China). Anti-mouse IgD antibodies were purchased from eBioscience (San Diego, CA, USA).

Samples collection, Jurkat cell line, and animals

The study protocol was carried out in accordance with the Declaration of Helsinki and approved by the Ethics Committee of Anhui Medical University (Nos. 20160119 and 20160095). Peripheral blood samples from healthy donors and RA patients were collected from the First Affiliated Hospital, Anhui Medical University. Written informed consent was obtained from all participants before enrollment in the study in accordance with the Declaration of Helsinki, and all donor samples were made anonymous to maintain health information confidentiality. Jurkat and Clone E6-1 cells were obtained from Procell Life Science & Technology Co., Ltd., and cultured according to their guidelines. Seven-week-old male DBA/1 mice (18 ± 2 g) (Certificate No. 11400700370327) were obtained from Beijing Wei Tong Li Hua Laboratory Animal Technology Co., Ltd., and maintained in a specific pathogen-free animal laboratory at Anhui Medical University.

Isolation of human CD4⁺ T cells and CD19⁺ B cells

PBMCs were isolated from the peripheral blood of healthy controls and RA patients by Ficoll gradient centrifugation. PBMCs were stained with the following fluorescently labeled mAbs against surface molecules: FITC antihuman CD4 (Cat. No. 555346, BD, NJ, USA) and PerCP-cy5.5 antihuman CD19 (Cat. No. 555414, BD, NJ, USA). CD4⁺ T cells and CD19⁺ B cells were sorted and collected by a flow cytometer (BD FACSAria™ II, BD, NJ, USA). Preparations were typically > 95% pure.

Coculture of human CD4⁺ T cells and CD19⁺ B cells

CD4⁺ T cells and CD19⁺ B cells from the PBMCs of healthy controls and RA patients were cocultured in RPMI 1640 with 10% fetal bovine serum (HyClone, Carlsbad, CA, USA) in Transwell chambers (0.4 μ m pore size/24-well plates); CD4⁺ T cells (1 × 10⁶ cells/well) were seeded in the lower chambers, and CD19⁺ B cells (1 × 10⁶ cells/well) were seeded in the upper chambers. CD4⁺

T cells were cultured with increasing concentrations of IgD (1, 3, and 10 μ g/mL) (Cat. No. ab91022, Abcam, Cambridge, UK) or IgD (3 μ g/mL) with different concentrations of IgD-Fc-Ig fusion protein (3, 10 μ g/mL), Lck inhibitor A770041 (0.5 μ M), and IgG₁-Fc (10 μ g/mL). B cells in the absence of T cells were set as the control group, and T cells and B cells without any treatment were set as the T-cell + B-cell group. Each treated group was cocultured with CD19⁺ B cells simultaneously for 24 or 48 h at 37 °C.

Biotin labeling of IgD protein

The primary antibody for biotin-labeled IgD was prepared, and the human IgD protein was labeled with biotin according to the instructions of the biotin labeling -NH₂ kit (Cat. No. LK03, DOJINDO, Japan), and the labeled protein was stored at -20 °C.

Immunofluorescence confocal microscopy analysis

Pretreated CD4⁺ T cells were fixed with 4% paraformaldehyde for 15 min and rinsed three times with PBS for 10 min each. The cells were permeabilized with 0.1% Triton X-100 solution at room temperature and then rinsed with PBS three times. The cells were blocked for 1 h in a 37 °C incubator with 10% occluded sheep serum. The serum was discarded, and then the primary antibody to phosphorylated Lck (p-Lck) (Tyr394) (rabbit, Cat. No. GTX133876, Gene Tex, KS, USA) at a 1:1000 ratio and primary antibody to biotin-labeled IgD at a 1:25 ratio were stored at 4 °C overnight. The primary antibody was then discarded and rinsed three times with PBS. Fluorescent secondary antibody, Alexa Fluor 488-conjugated goat anti-mouse IgG (Cat. No. FMS-Msaf48801, Fcmacs, China) and PE-cy7 streptavidin (Cat. No. 405206, Biolegend, CA, USA), was incubated at a 1:100 ratio in a 37 °C incubator for 1 h in the dark. The fluorescent secondary antibody was then discarded and rinsed three times with PBS. Nuclei were stained with DAPI staining solution for 10 min and rinsed four times with PBS. Images were acquired on a Leica SP8 TCS STED ×3 confocal microscope system (Leica, Germany) with an HC PL APO ×100/1.4 NASTED objective (IgDR and p-Lck).

Quantification of colocalization

The images were analyzed with the "Colocalization Module" of a Leica SP8 TCS STED ×3 microscope system. The colocalization index of IgDR and p-Lck was determined through the colocalization rate, Pearson's correlation, and overlap coefficient. Background correction in manual mode was performed and kept consistent for all images that were compared to confirm colocalization of IgDR and p-Lck on CD4⁺ T cells.

Coimmunoprecipitation (Co-IP) analysis

Pretreated CD4⁺ T cells plated in six-well plates (5 × 10⁶/well) were centrifuged at 800 × g for 10 min for collection in 1.5 mL EP tubes, and then 200 μ L of lysate was added to each tube. Cells were suspended to lyse the cells and shaken on ice for 30 min. The cells were centrifuged at 13,400 × g for 15 min at 4 °C, and then the supernatant was extracted on ice. Homologous IgG antibody (rabbit, Cat. No. sc-2025 Santa Cruz Blotechnology, CA, USA) was added at a ratio of 1:500 along with A/G agarose beads (1:50) (Cat. No. sc-2003, Santa Cruz Blotechnology, CA, USA). This was followed by centrifugation at 4 °C for 15 min. The supernatant was collected at 15,000 × g. Then, A/G agarose beads were added again (1:100), and the p-Lck (Tyr394) primary antibody (1:1000) was added at 4 °C overnight. The agarose beads were then rinsed three times with 1 × IP buffer. Each time, the agarose beads were collected by centrifugation at 3000 × g for 5 min in a 4 °C centrifuge, 50 μ L of 1 × IP buffer was added to the agarose bead binding protein, and the loading buffer was added at a ratio of 1:4 and then boiled for 8 min after 10% SDS-page analysis. The membrane was scanned on a GS-700 Imaging Densitometer. The image was analyzed with ImageJ software (1.43.67).

Activation and immunofluorescence-based detection of NF- κ B nuclear translocation

Jurkat cells (2×10^6 cells/mL) in the exponential growth phase were treated with $3 \mu\text{g/mL}$ IgD. IgD-induced Jurkat cells were incubated with $10 \mu\text{g/mL}$ IgD-Fc-Ig and $0.5 \mu\text{M}$ Lck inhibitor A770041 for 4 h in dishes with a diameter of 34.8 mm. Cells in dishes were centrifuged at $800 \times g$ for 10 min for collection, followed by incubation with cytoperm/cytofix buffer for 30 min and washing with PBS. After washing, the cells were incubated for 30 min with PE antihuman phospho-transcription factor NF- κ B p65 (Ser529) (Cat. No. 2038939, Invitrogen-Thermo Fisher Scientific, MA, USA) and washed with PBS. After washing, the DNA-binding dye DAPI (Cat. No. C1005, Beyotime, China) was added for 30 min, and the samples were then washed and suspended in PBS. The samples were run directly on the Image Stream system (ImageStream^X Mark II, Germany), and all fixation and staining reactions were carried out on ice in the dark. All washes were performed with cold PBS.

Image stream data acquisition and analysis

The fluorescence image-based method for quantifying nuclear translocation described here relies on the differential spectral isolation of NF- κ B and DAPI images from nuclear images with Image Stream technology [14]. Determination of NF- κ B translocation from a similarity score [14]: the assessment of nuclear translocation was performed in a qualitative manner by comparing a cell's nuclear fluorescence (DAPI fluorescence) image to the pattern of fluorescence produced by the NF- κ B label (PE). Nuclear translocation was judged to have occurred if the NF- κ B and nuclear fluorescence signals overlapped with similar shapes. Conversely, if the NF- κ B signal surrounded the nucleus, it was judged not to exhibit significant translocation. The similarity score is a method of quantitatively performing this assessment. The similarity score has a high positive value if the NF- κ B and nuclear images are alike. In contrast, if the NF- κ B and image are dim where the nuclear image is bright, the score has a large negative value. The data pairs are the pixel intensities of the two different fluorescence intensities at the same location in each image. Plotting the pixel intensities of the nuclear image against the transcription factor image reveals an inverse correlation for untranslocated protein and a positive correlation for translocated protein in a cell

Cell counting kit-8 (CCK-8) analysis

CD4⁺ T cells and CD19⁺ B cells from RA patients were treated and cocultured as described previously. CD4⁺ T cells were cultured in the presence or absence of increased concentrations of IgD (1, 3, and $10 \mu\text{g/mL}$). The control and T-cell + B-cell groups were set as previously described. To assess the proliferative responses of cultured cells, a CCK-8 (Cat. No. CK04, DOJINDO, Japan) assay was used to explore the viability of CD19⁺ B cells after coculture for 24 and 48 h. $100 \mu\text{L}$ per well of CD19⁺ B cells in the upper chamber was collected and seeded in triplicate in 96-well round-bottom microtiter wells. Then, $10 \mu\text{L}$ of CCK-8 solution was added per well. The cells were incubated for 4 h at 37°C in an atmosphere containing 5% CO_2 , and the absorbance at 450 nm was measured on a microplate reader (Infinite M1000 PRO, TECAN, Switzerland).

Flow cytometry analysis

After 48 h of coculture, CD4⁺ T cells were harvested from chambers at the end of the incubation period and stained for 30 min on ice with antigen-presenting cell (APC) antihuman CD40L (CD154) (Cat. No. 310809, Biolegend, CA, USA). CD19⁺ B cells were harvested from chambers at the end of the incubation period and stained for 30 min on ice with BV421-CD40 (Cat. No. 334332, Biolegend, CA, USA) and PE antihuman CD86 (Cat. No. 305405, Biolegend, CA, USA). For each sample, 20,000 cells were collected, and as a result, the density of the dot plots reveals

relative cell numbers. The median fluorescence intensity (MFI) of CD40L, CD40, and CD86 expression was determined via flow cytometry (Beckman Coulter, Beckman Coulter Biotechnology, CA, USA) and analyzed with CytExpert (2.1.0.92).

Induction and treatment of CIA mice

A type II collagen sample was dissolved in acetic acid (0.1 mol/L) at 2 mg/mL and incubated overnight at 4°C . The sample was then emulsified with an equal volume of complete Freund's adjuvant. Arthritis was induced in 7-week-old male DBA/1 mice by intradermal injection of 0.15 mL of CII emulsion into the base of the tail, followed by a booster injection of 0.1 mL of emulsion on day 21. Mice were maintained in a specific pathogen-free animal laboratory at Anhui Medical University. The mice were divided into nine treatment groups: normal, CIA model, IgD-Fc-Ig (1.625, 3.25, 6.5, and 13 mg/kg), IgG₁-Fc (13 mg/kg), rhTNFR:Fc (4.5 mg/kg), and anti-mouse IgD antibody (2 mg/kg). After the onset of arthritis at day 30, the mice were treated with IgD-Fc-Ig, IgG₁-Fc, or rhTNFR:Fc through intravenous tail injection (twice weekly, for 4 weeks), and anti-IgD antibody (once daily, for 3 days). rhTNFR:Fc and anti-IgD antibody treatment groups were used as positive controls. The mice in the normal control group were treated with an equal volume of saline by intravenous injection. Mice were sacrificed on day 54, and spleens were collected for immunohistochemistry (IHC) analysis.

Mice splenocyte isolation and coculture

Mouse spleens were pressed and washed through a 200-gauge mesh. Splenocytes were isolated by Ficoll gradient centrifugation. Splenocytes were stained with fluorescently labeled mAbs against surface molecules such as FITC anti-mouse CD4 (Cat. No. 553047, BD, NJ, USA) and PE-cy5 anti-mouse CD19 (Cat. No. 552854, BD, NJ, USA). CD4⁺ T cells and CD19⁺ B cells were sorted and cocultured as described previously.

Western blot analysis

For the in vitro study, CD4⁺ T cells and CD19⁺ B cells from PBMCs of healthy controls and RA patients were collected after T-B-cell coculture. Cells were lysed in lysis buffer supplemented with protease inhibitors and phosphatase inhibitors for 30 min on ice. In an animal study, CD4⁺ T cells and CD19⁺ B cells from splenocytes of CIA mice were collected and lysed after T-B-cell coculture. Primary antibodies against Lck (rabbit, 1:1000, Cat. No. GTX107785, Gene Tex, KS, USA), p-Lck (Tyr394) (rabbit, 1:1000, Cat. No. GTX133876, Gene Tex, KS, USA), ZAP70 (rabbit, 1:500, Cat. No. AF6312, Affinity, China), p-ZAP70 (rabbit, 1:500, Cat. No. AF3312, Affinity, China), PI3K (rabbit, 1:1000, Cat. No. 4257T, Cell Signaling, Germany), p-PI3K (rabbit, 1:1000, Cat. No. 4228T, Cell Signaling, Germany), CD40L (rabbit, 1:500, Cat. No. DF2301, Affinity, China), CD40 (rabbit, 1:500, Cat. No. AF5336, Affinity, China), and β -actin (mouse, 1:1000, Cat. No. 66009-Ig, proteintech, USA) were then incubated at 4°C overnight, and goat anti-rabbit (1:1000, Cat. No. 7074P2, Cell Signaling, Germany)/mouse conjugated secondary antibodies (1:1000, Cat. No. SA00001-1, Proteintech, USA) were incubated for 2 h at 37°C . The membrane was scanned on a GS-700 Imaging Densitometer. The image was analyzed with ImageJ software (1.4.3.67).

Immunohistochemistry (IHC)

The spleens of each mouse group were dehydrated ($2 \times 70\%$ EtOH, $2 \times 90\%$ EtOH, $2 \times 100\%$ EtOH, $3 \times 100\%$ xylene, $3 \times$ paraffin; each 90 min), embedded in paraffin in plastic holders, and then prepared as $5 \mu\text{m}$ paraffin microtome slices. After blocking with 2% BSA/PBS, sections were labeled with primary antibodies against CD40, CD40L, and IgD. Detection of primary antibodies was performed using goat anti-rabbit conjugated secondary antibodies and peroxidase-based detection systems using the ABC complex and DAB as substrate. Images were acquired on an Olympus BX53F microscope system (Olympus, Japan) with a $\times 40$ objective.

ELISA

The levels of IL-17A were determined in serum samples and cellular supernatant samples using ELISA (Cat. No. ab100702, Abcam, Cambridge, UK) according to the manufacturer's instructions. The ODs of each sample were detected at 450 nm with an Infinite M1000 PRO microplate reader.

Statistical analysis and quantification

In this study, SPSS 16.0 was used for the statistical analysis, and the two groups were compared using the *t*-test. Data are presented as the mean \pm standard error (SEM), and calculations completed using Prism 6 software with two-way ANOVA multiple comparison tests. $P < 0.05$ was considered statistically significant.

RESULTS

Effects of IgD-Fc-Ig on the coexpression of IgDR and Lck in human CD4⁺ T cells

We used immunofluorescence confocal microscopy and Co-IP methods to examine the coexpression of IgDR and p-Lck proteins on CD4⁺ T cells in healthy controls. Confocal microscopy results clearly showed that IgDR fluorescence (red) on CD4⁺ T cells occurred in the same area as p-Lck fluorescence (green), proving the interaction of the two molecules (Fig. 1a). The colocalization rate, Pearson's correlation and overlap coefficient were used to quantify colocalization. The colocalization rate (%) showed that the red-green pair implies that all red pixels colocalized with green. Pearson's correlation described the correlation of the intensity distribution between channels (ranging from -1.0 to 1.0 ; 0 indicates no significant correlation and -1.0 indicates a complete negative correlation). The overlap coefficient splits the value of colocalization into two separate parameters, allowing the determination of the contribution of each antigen to the areas with colocalization. Our results showed that in these colocalization coefficient graphs IgD (3 μ g/mL) significantly promoted the coexpression of IgDR and p-Lck on CD4⁺ T cells (Fig. 1b–d) compared to the control group ($P < 0.01$). IgD-Fc-Ig (10 μ g/mL) and the Lck inhibitor A770041 (0.5 μ M) significantly decreased the coexpression of IgDR and p-Lck (Fig. 1b–d) compared to that in the IgD (3 μ g/mL) stimulation group ($P < 0.01$).

The results of Co-IP were consistent with those of laser confocal microscopy. IgD (3 μ g/mL) significantly promoted the coexpression of IgDR and p-Lck on CD4⁺ T cells (Fig. 1e) compared to that in the control group ($P < 0.05$). IgD-Fc-Ig (10 μ g/mL) and the Lck inhibitor A770041 (0.5 μ M) significantly decreased the coexpression of IgDR and p-Lck (Fig. 1e) compared to that in the IgD (3 μ g/mL) stimulation group ($P < 0.05$).

Effects of IgD-Fc-Ig on the protein expression of p-Lck, ZAP70, p-ZAP70, PI3K, p-PI3K in CD4⁺ T cells from healthy controls

The expression levels of p-Lck, ZAP70, p-ZAP70, PI3K, and p-PI3K were analyzed by Western blotting. No significant differences were observed in the total protein expression of ZAP70 and PI3K between the treatment groups (Fig. 2a). The expression levels of p-Lck, p-ZAP70, and p-PI3K were obviously increased in CD4⁺ T cells stimulated with IgD (3 and 10 μ g/mL) compared to those in the control group ($P < 0.01$). Treatment with both IgD-Fc-Ig (10 μ g/mL) and the Lck inhibitor A770041 (0.5 μ M) significantly reduced the expression of p-Lck, p-ZAP70, and p-PI3K (Fig. 2b–d) compared to that in the IgD (3 μ g/mL) stimulation group ($P < 0.01$).

Effects of IgD-Fc-Ig on NF- κ B nuclear translocation stimulated by IgD in Jurkat cells

NF- κ B nuclear translocation was monitored and quantitated using the similarity score with Image Stream technology, as described in the "Materials and Methods" (Fig. 3a, b). We observed that the optimal stimulation time point was 4 h (Supplementary data). Fig. 3b1 presents Image Stream images of four control cells,

Fig. 3b2 presents Image Stream images of four IgD-induced cells, Fig. 3b3 presents Image Stream images of four IgD-induced cells incubated with IgD-Fc-Ig, Fig. 3b4 presents Image Stream images of four IgD-induced cells incubated with the Lck inhibitor A770041. Stimulation of Jurkat cells with 3 μ g/mL IgD clearly resulted in nuclear translocation of NF- κ B within 4 h, as expected, as measured by the G-mean (Fig. 3c) compared to the control group ($P < 0.01$). In addition, IgD-induced cells incubated with IgD-Fc-Ig (10 μ g/mL) and the Lck inhibitor A770041 (0.5 μ M) revealed a decrease in NF- κ B nuclear translocation (Fig. 3c) compared to that in the IgD (3 μ g/mL) stimulation group ($P < 0.01$).

Effects of IgD-activated CD4⁺ T cells on CD19⁺ B cells in healthy controls

To confirm the effect of IgD-induced CD4⁺ T cells on CD19⁺ B-cell proliferation and activation in healthy controls, CD19⁺ B cells were cocultured with IgD (3 μ g/mL)-treated CD4⁺ T cells or CD19⁺ B cells treated with IgD (3 μ g/mL) in vitro for 24 and 48 h, and the proliferation of CD19⁺ B cells was measured. IgD-activated CD4⁺ T cells caused the proliferation of CD19⁺ B cells ($P < 0.01$), while CD19⁺ B cells directly stimulated by IgD did not show B-cell proliferation (Fig. 4a, b). The expression of CD40L on CD4⁺ T cells and CD40 on CD19⁺ B cells, which were used to indicate the activation of T and B cells, was analyzed by Western blotting and flow cytometry after coculture. The Western blotting results showed that the expression of CD40L on CD4⁺ T cells was upregulated after IgD (3 and 10 μ g/mL) treatment (Fig. 4c) compared to the control treatment ($P < 0.01$). In addition, the expression of CD40 on CD19⁺ B cells (Fig. 4d) was upregulated after coculture with IgD-activated CD4⁺ T cells ($P < 0.01$). In addition, the flow cytometry results showed the same trend: the expression of CD40L on CD4⁺ T cells was upregulated after IgD (3, 10 μ g/mL) treatment (Fig. 4e) compared to the control treatment ($P < 0.05$), and the expression of CD40 on CD19⁺ B cells (Fig. 4f) was upregulated after coculture with IgD-activated CD4⁺ T cells ($P < 0.001$).

Effects of IgD-Fc-Ig on IgD-activated CD4⁺ T cells in RA patients Human CD4⁺ T cells activated by IgD have been shown to induce B-cell activation from peripheral blood in healthy controls. Then, we extended this result to demonstrate the effect of IgD-Fc-Ig on the coculture of IgD-activated CD4⁺ T cells and CD19⁺ B cells from RA patients. To confirm this finding in healthy controls, we observed the effect of IgD-activated CD4⁺ T cells on CD19⁺ B-cell proliferation and activation. CD4⁺ T cells were incubated with different concentrations of IgD (1, 3, 10 μ g/mL) and cocultured with CD19⁺ B cells in vitro for 24 and 48 h, and the proliferation of CD19⁺ B cells was measured. As expected, IgD (1, 3, 10 μ g/mL)-activated CD4⁺ T cells increased the proliferation of CD19⁺ B cells in a concentration-dependent manner ($P < 0.05$) (Fig. 5a, b). The expression levels of CD40L on CD4⁺ T cells and CD40 on CD19⁺ B cells were analyzed separately. Consistent with the finding obtained in healthy controls, the Western blotting results showed that expression of CD40L on CD4⁺ T cells were upregulated after IgD (3, 10 μ g/mL) treatment (Fig. 5c) compared to the control treatment ($P < 0.01$). In addition, the expression of CD40 on CD19⁺ B cells (Fig. 5d) was upregulated after coculture with IgD-activated CD4⁺ T cells ($P < 0.01$). The upregulated expression of CD40L on CD4⁺ T cells induced by IgD (3 μ g/mL) stimulation was downregulated by IgD-Fc-Ig (3 and 10 μ g/mL) treatment ($P < 0.01$). Moreover, the expression of CD40 on CD19⁺ B cells was downregulated by the same treatment after T–B-cell coculture (Fig. 5e, f).

The flow cytometry results showed the same trend, and the expression of CD40L on CD4⁺ T cells was upregulated after IgD (3, 10 μ g/mL) treatment (Fig. 5g) compared to the control treatment ($P < 0.01$). In addition, the expression of CD40 on CD19⁺ B cells (Fig. 5h) was upregulated after coculture with IgD-activated CD4⁺ T cells ($P < 0.001$). The upregulated expression of CD40L on CD4⁺

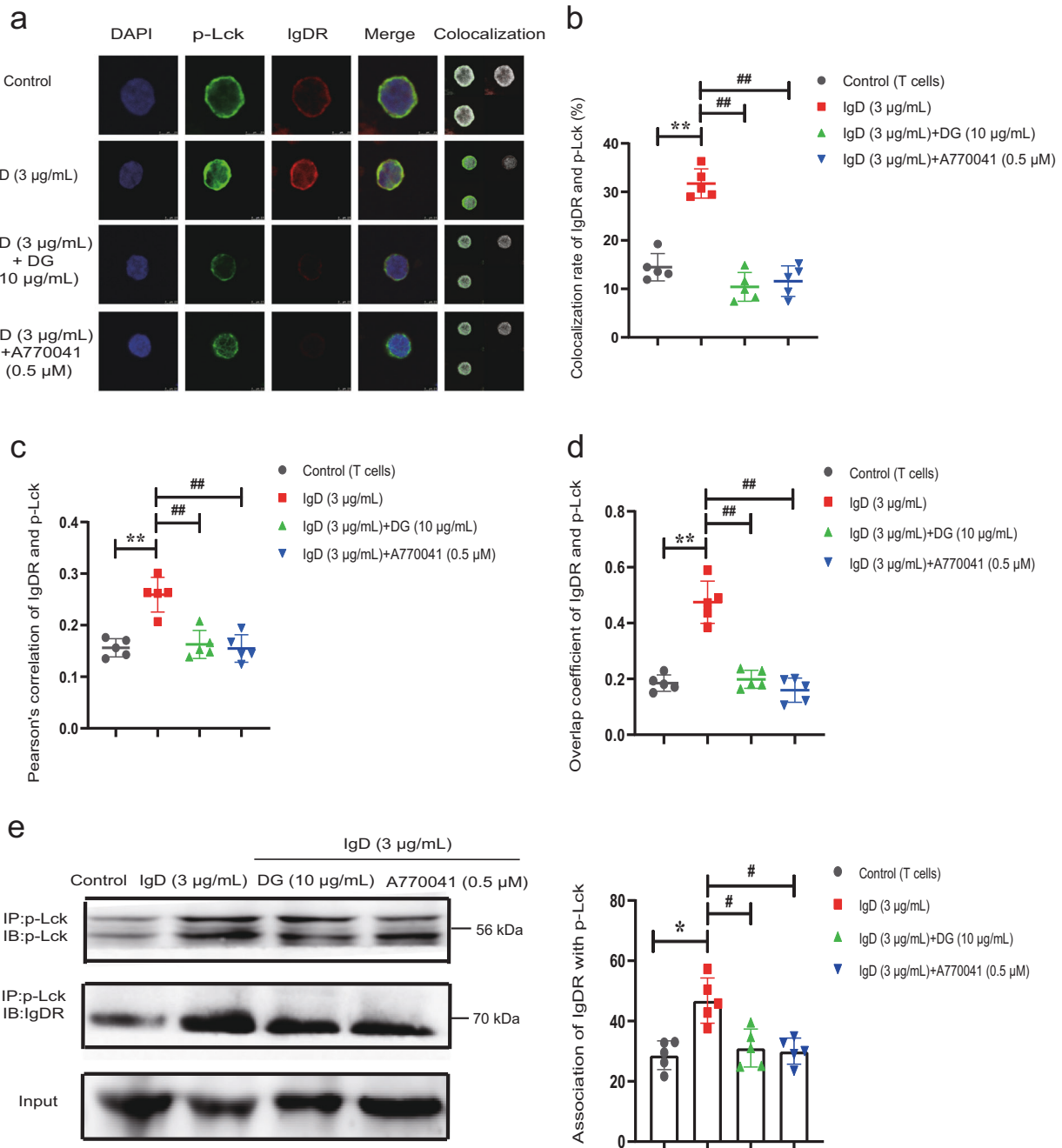


Fig. 1 Effects of IgD-Fc-Ig (DG) on the IgDR-p-Lck interaction on CD4⁺ T cells in healthy controls induced by IgD. To obtain CD4⁺ T cells from PBMCs of healthy controls, CD4⁺ T cells were incubated with IgD (3 µg/mL), IgD-Fc-Ig (10 µg/mL), and 0.5 µM Lck inhibitor (A770041) for 24 h. **a** Confocal microscopy of CD4⁺ T cells stained for IgDR and p-Lck: red, staining of CD4⁺ T cells with labeled IgDR protein; green, staining of CD4⁺ T cells with labeled p-Lck protein; blue, staining of nuclei with the DNA-binding dye DAPI. **b** Colocalization rate of IgDR and p-Lck proteins (%). **c** Pearson's correlation of IgDR and p-Lck proteins. **d** Overlap coefficient of IgDR and p-Lck proteins. Data were analyzed by the "Colocalization Module" of a Leica SP8 TCS STED \times 3 microscope system and are expressed as the mean \pm SEM ($n = 5$). ****** $P < 0.01$ vs. control (T cells), **##** $P < 0.01$ vs. IgD (3 µg/mL) stimulation group. **e** Coimmunoprecipitation analysis of IgDR-p-Lck interactions on CD4⁺ T cells in healthy controls. Data were expressed as the mean \pm SEM ($n = 5$). ***** $P < 0.05$ vs. control (T cells), **#** $P < 0.05$ vs. IgD (3 µg/mL) stimulation group.

T cells by IgD (3 µg/mL) stimulation was downregulated by IgD-Fc-Ig (3 and 10 µg/mL) treatment (Fig. 5i) ($P < 0.001$). In addition, the expression of CD40 on CD19⁺ B cells was downregulated by the same treatment after T-B-cell coculture (Fig. 5j) ($P < 0.001$). Moreover, the effect of IgD-Fc-Ig on CD86 expression on CD19⁺ B cells was analyzed by FCM. The expression of CD86 was upregulated after IgD (10 µg/mL) treatment (Fig. 5k) compared to the T-cell + B-cell treatment ($P < 0.05$). The upregulated expression of CD86 on CD19⁺ B cells induced by IgD (10 µg/mL) stimulation

was downregulated by IgD-Fc-Ig (3 and 10 µg/mL) treatment ($P < 0.05$) (Fig. 5k).

Effects of IgD-Fc-Ig on the expression of CD40, CD40L, and IgD in CIA mice

We established the CIA model, and mice were treated with IgD-Fc-Ig, IgG1-Fc, rhTNFR:Fc, or anti-IgD antibody through tail intravenous injection. To observe the effect of IgD-Fc-Ig on the overall mouse model, the expression of CD40, CD40L, and IgD in mouse spleens

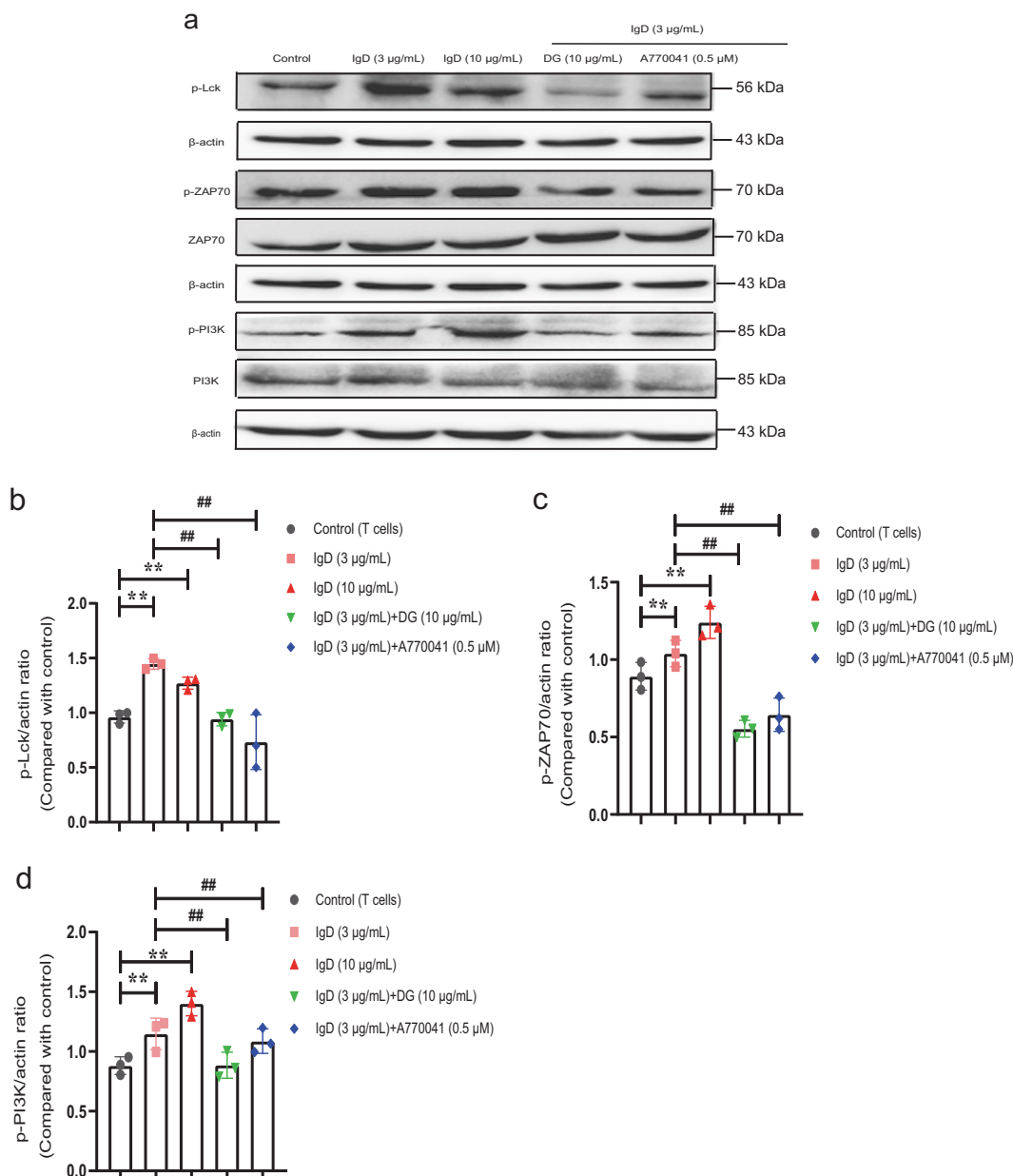


Fig. 2 Effects of IgD-Fc-Ig (DG) on the protein expression of p-Lck, ZAP70, p-ZAP70, PI3K, and p-PI3K. Western blot analysis (a) of p-Lck (b), ZAP70, p-ZAP70 (c), PI3K, and p-PI3K (d) expression on CD4⁺ T cells from PBMCs of healthy controls. CD4⁺ T cells were incubated with IgD (3, 10 µg/mL), DG (10 µg/mL), and 0.5 µM Lck inhibitor A770041 for 24 h and lysed. Data were expressed as the mean \pm SEM ($n = 3$). ** $P < 0.01$ vs. control, ## $P < 0.01$ vs. IgD (3 µg/mL) stimulation group.

was analyzed by IHC. The expression levels of CD40, CD40L, and IgD in spleens from CIA mice were higher than those in spleens from normal mice ($P < 0.01$). Etanercept (4.5 mg/kg) and anti-mouse IgD antibody (2 mg/kg) administration downregulated the expression of CD40, CD40L, and IgD in CIA mouse spleens ($P < 0.01$). IgD-Fc-Ig (3.25, 6.5, 13 mg/kg) administration dose-dependently downregulated the expression of CD40, CD40L, and IgD in spleens ($P < 0.05$). In contrast, the expression of CD40, CD40L, and IgD in the IgG₁-Fc (13 mg/kg) administration group did not undergo efficient changes compared to the CIA mouse group (Fig. 6a–c).

Effects of IgD-Fc-Ig on IgD-activated CD4⁺ T cells in CIA mice in vitro

To identify the effect of IgD-Fc-Ig on the coculture of IgD-activated CD4⁺ T cells and CD19⁺ B cells in CIA mice, the expression levels

of CD40L on CD4⁺ T cells and CD40 on CD19⁺ B cells from the spleens of CIA mice were analyzed by Western blotting. Consistent with the finding obtained in human samples, the expression of CD40L on CD4⁺ T cells was upregulated after IgD (3 µg/mL) treatment (Fig. 7a) compared to the control treatment ($P < 0.01$). In addition, the expression of CD40 on CD19⁺ B cells (Fig. 7b) was upregulated after coculture with IgD-activated CD4⁺ T cells ($P < 0.01$). The upregulated expression of CD40L on CD4⁺ T cells induced by IgD (3 µg/mL) stimulation could be downregulated by IgD-Fc-Ig (10 µg/mL) treatment or Lck inhibitor A770041 treatment (0.5 µM) ($P < 0.01$). In addition, the expression of CD40 on CD19⁺ B cells was downregulated by the same treatments after T–B-cell coculture (Fig. 7a, b). IgG₁-Fc (10 µg/mL) treatment did not induce strong changes in the expression of CD40L and CD40 (Fig. 7a, b).

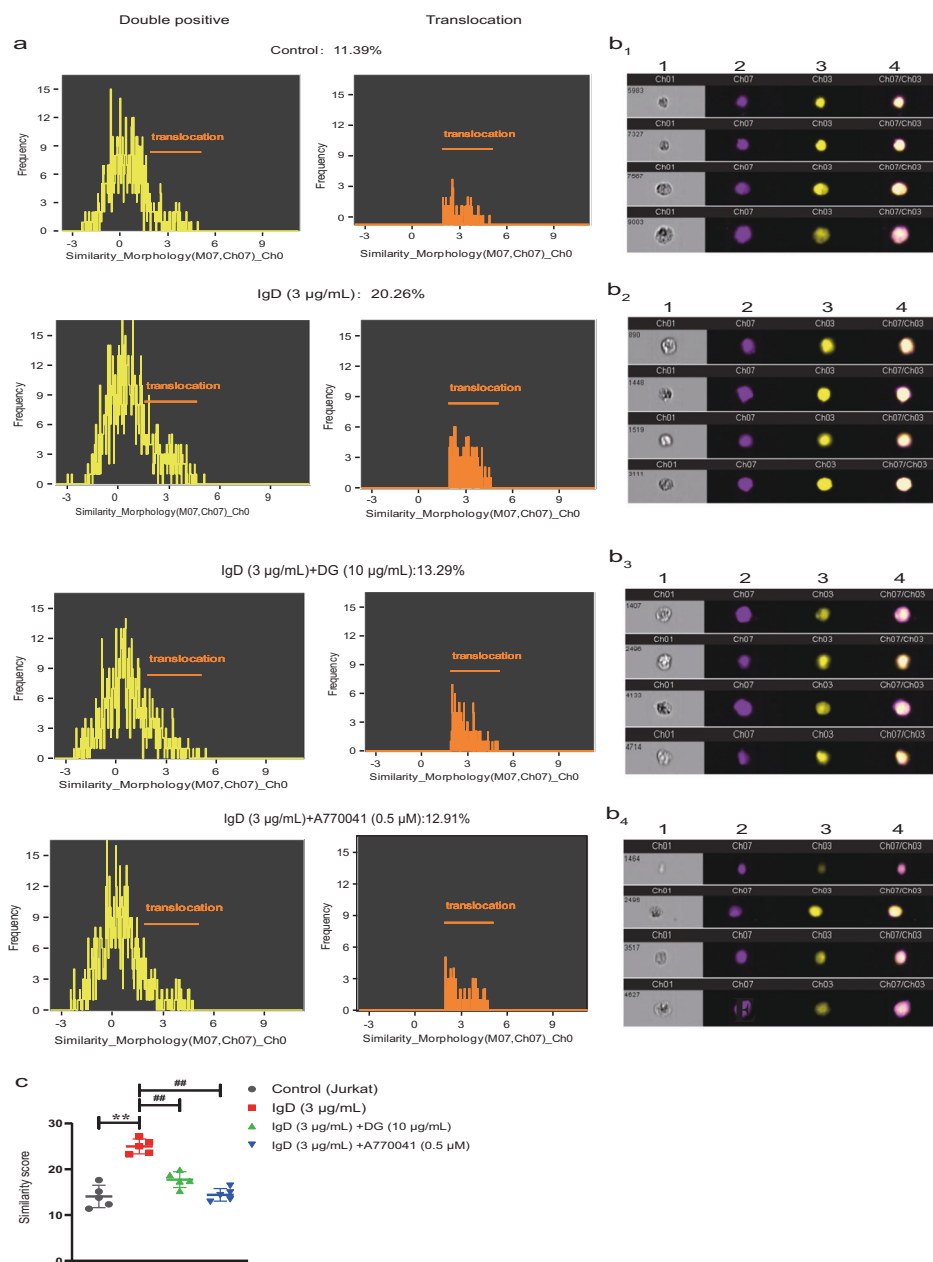


Fig. 3 Image Stream fluorescence imaging of NF- κ B nuclear translocation in Jurkat cells after IgD induction and incubation with IgD-Fc-Ig (DG) and the Lck inhibitor A770041. **a** Quantification of nuclear translocation using the similarity algorithm. The region High Sim drawn on the dark field/DAPI similarity plot represents the region for positive image correlation for the similarity algorithm. This region is applied to the NF- κ B/DAPI similarity plot. The percentages of cells that fall within the High Sim region are displayed on the right of each histogram. **b** Control unstimulated Jurkat cells (b₁), Jurkat cells treated with 3 μ g/mL IgD for 4 h (b₂), and IgD-induced Jurkat cells incubated with 10 μ g/mL DG (b₃) and 0.5 μ M Lck inhibitor A770041 (b₄) for 4 h were probed for NF- κ B expression and DAPI as described in the “Materials and Methods” and run on the Image Stream. The multispectral imaging system acquires up to six images per cell in three different imaging modes: bright field (morphology) (1) and fluorescence: Ch07-DAPI (purple) (2), Ch03-NF- κ B (yellow-PE) (3), and NF- κ B/DAPI composite images (4) for five representative (of 10,000 images) cells and are shown for each treatment group. Pixel intensities from the NF- κ B images are plotted against the corresponding pixel intensities from the DAPI or dark-field images. **c** NF- κ B nuclear translocation in Jurkat cells. The G-means represents the geometric means of the similarity of the nuclear/cytoplasmic NF- κ B intensity ratio to DAPI intensity. Jurkat cells were either left unstimulated or stimulated with IgD 3 μ g/mL. IgD-induced Jurkat cells were incubated with 10 μ g/mL DG and 0.5 μ M Lck inhibitor A770041. The results show the mean \pm SEM of five independent experiments in which the similarity ratio was calculated from 10,000 cells in each independent experiment. ** P < 0.01 vs. control, ## P < 0.01 vs. IgD (3 μ g/mL) stimulation group.

To determine the cytokine profile of IgD-activated T cells, the levels of IL-17A in CD4⁺ T cells from the culture supernatant following 48 h of coculture treatment were detected by ELISA. Substantial amounts of IL-17 were produced by IgD-activated T cells (Fig. 7c) compared to the control cells (P < 0.01). The

upregulated levels of IL-17A induced by IgD (3 μ g/mL) stimulation were downregulated by IgD-Fc-Ig (3 and 10 μ g/mL) treatment or Lck inhibitor A770041 treatment (0.5 μ M) (Fig. 7c) (P < 0.01). IgG₁-Fc had no significant effect on IL-17A secretion (Fig. 7c).

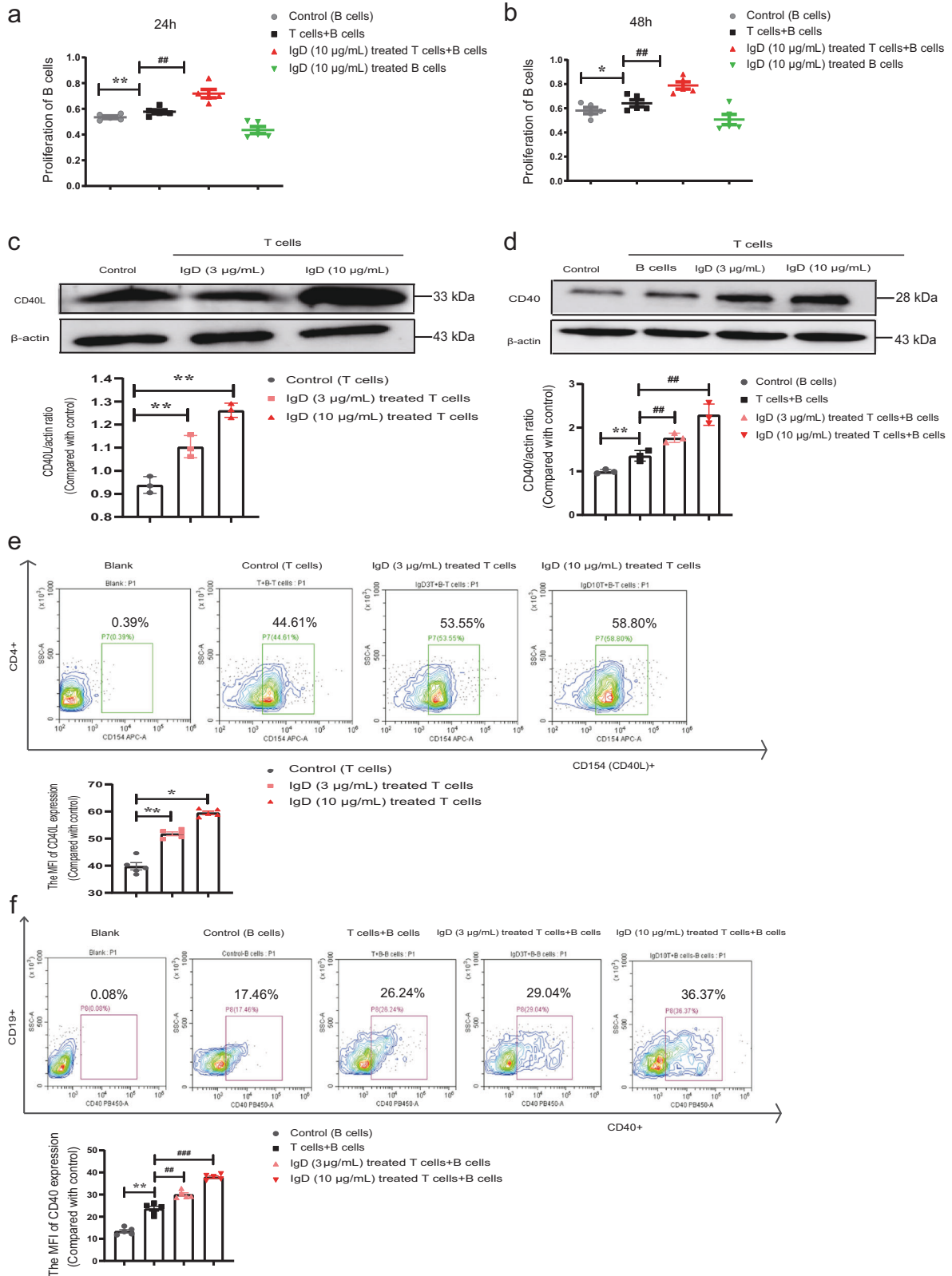


Fig. 4 Effects of IgD on CD4⁺ T-cell and CD19⁺ B-cell activities in healthy controls. Obtained CD4⁺ T cells and CD19⁺ B cells from PBMCs of healthy controls. CD4⁺ T cells were incubated with IgD (10 µg/mL) cocultured with CD19⁺ B cells in vitro for 24 and 48 h, and CD19⁺ B cells were incubated with IgD (10 µg/mL) in vitro for 24 and 48 h. **a, b** After coculture, CD19⁺ B cells were obtained, and CCK-8 analysis of the effect of IgD-induced CD4⁺ T cells on the proliferation of CD19⁺ B cells was performed. Western blot analysis of CD40L expression on CD4⁺ T cells (**c**) and CD40 expression on CD19⁺ B cells (**d**) from PBMCs of healthy controls. CD4⁺ T cells were incubated with IgD (3, 10 µg/mL), cocultured with CD19⁺ B cells in vitro for 48 h, and lysed. Flow cytometry analysis of CD40L expression on CD4⁺ T cells (**e**) and CD40 expression on CD19⁺ B cells after coculture (**f**). Data were expressed as the mean ± SEM (n = 5). *P < 0.05, **P < 0.01 vs. control; ##P < 0.01, ###P < 0.001 vs. T cells + B cells.

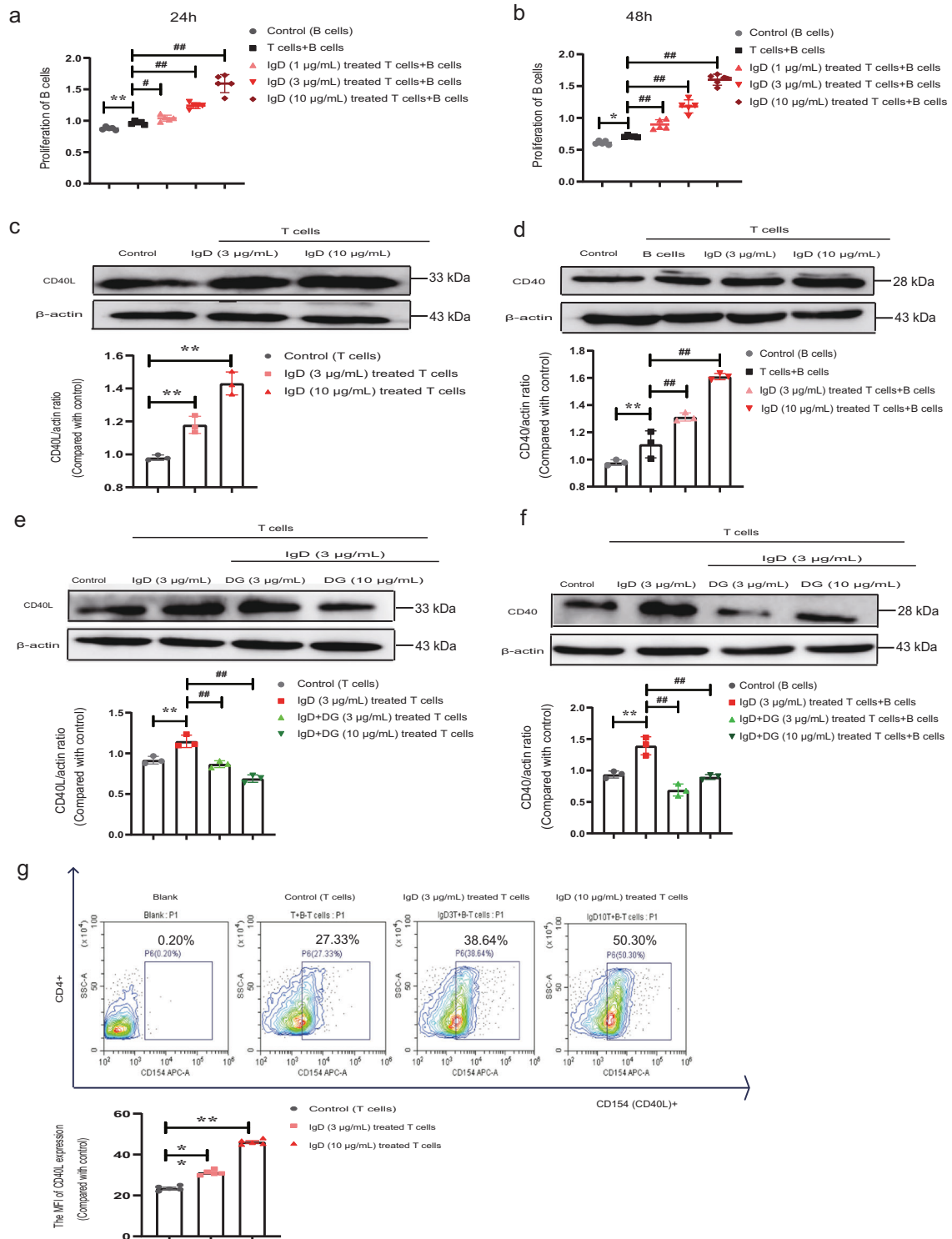


Fig. 5 (Continue)

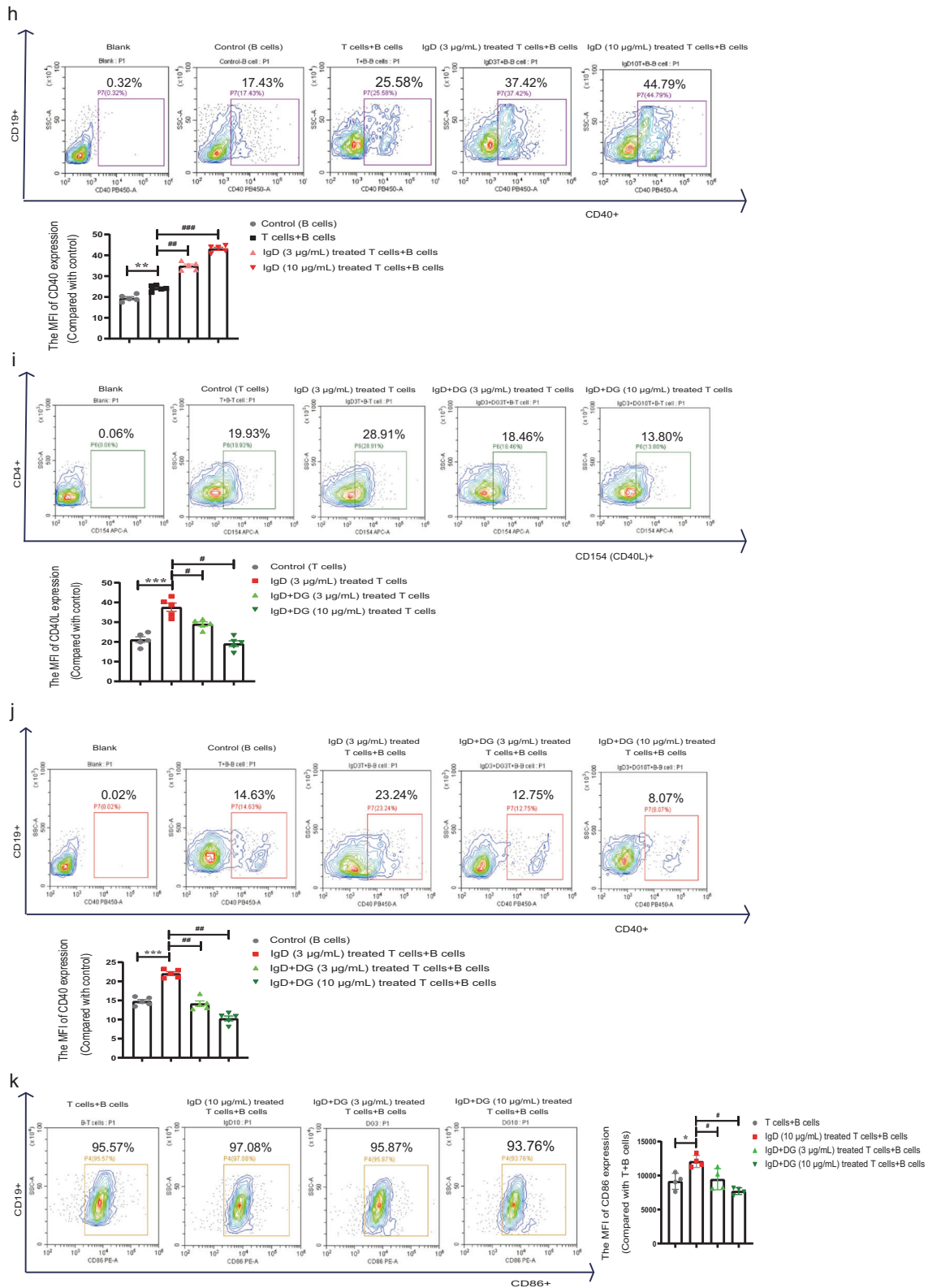


Fig. 5 Effects of IgD-Fc-Ig (DG) on CD4⁺ T-cell and CD19⁺ B-cell activities in RA patients. CD4⁺ T cells and CD19⁺ B cells were obtained from PBMCs of RA patients, and CD4⁺ T cells were incubated with different concentrations of IgD (1, 3, 10 μ g/mL) and DG (3, 10 μ g/mL) cocultured with CD19⁺ B cells in vitro for 24 h (a) and 48 h (b). After coculture, CD19⁺ B cells were obtained, and CCK-8 analysis of the effect of IgD-induced CD4⁺ T cells on the proliferation of CD19⁺ B cells was performed. After coculture, CD4⁺ T cells and CD19⁺ B cells were obtained and lysed. Western blot analysis of CD40L (c, e) and CD40 (d, f) expression on CD4⁺ T cells and CD19⁺ B cells from PBMCs of RA patients. Representative flow cytometry dot plot from each group. Flow cytometry analysis of CD40L (g, i) and CD40 (h, j) expression on CD4⁺ T cells and CD19⁺ B cells from PBMCs of RA patients. The MFI of CD86 expression on CD19⁺ B cells stimulated by IgD (k). Data were expressed as the mean \pm SEM ($n = 5$). * $P < 0.05$, ** $P < 0.01$, *** $P < 0.001$ vs. control, # $P < 0.05$, ## $P < 0.01$, ### $P < 0.001$ vs. T-B cells and IgD (3 μ g/mL) group and IgD (10 μ g/mL) stimulation group.

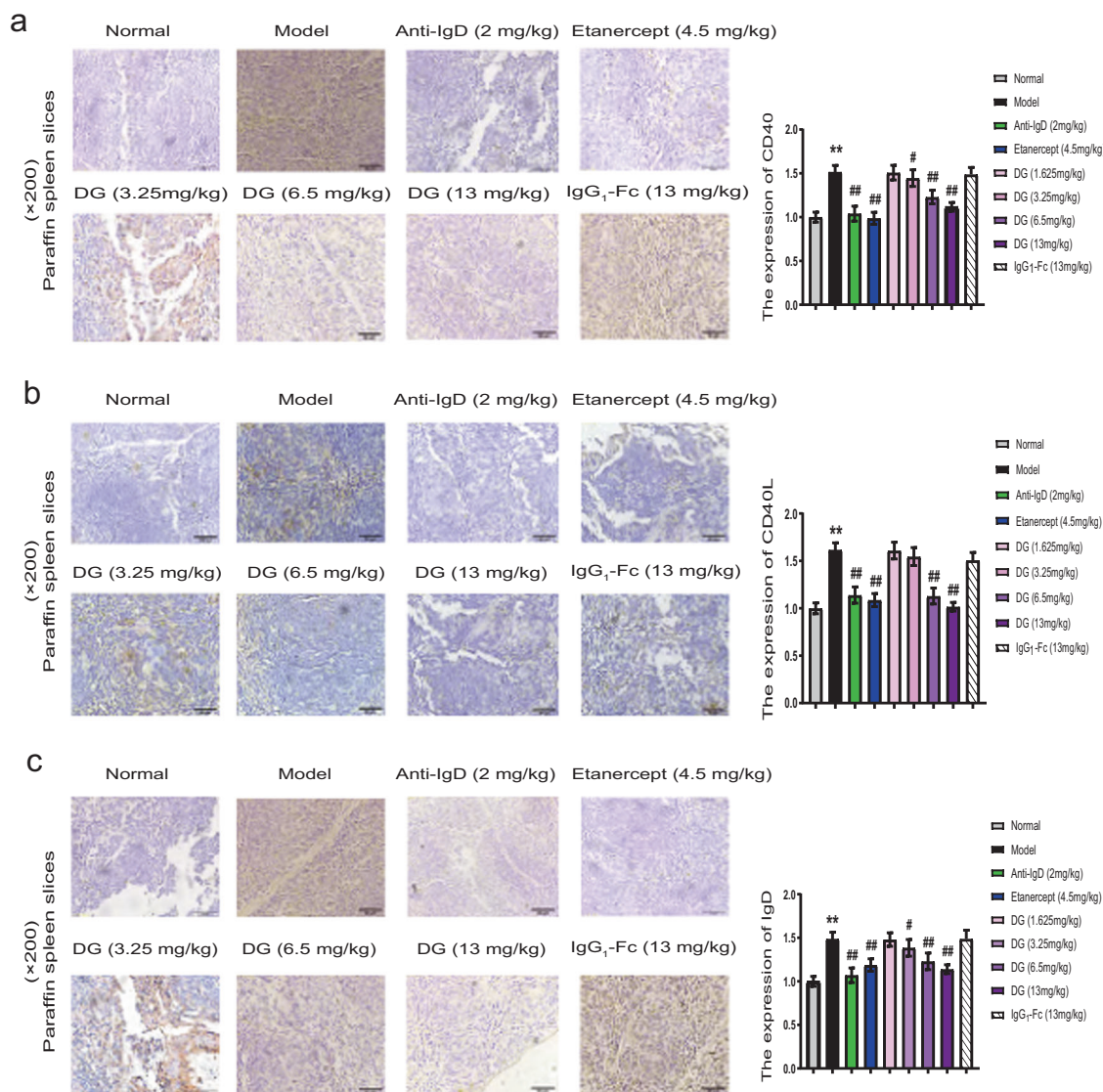


Fig. 6 Effects of IgD-Fc-Ig (DG) on CD40, CD40L, and IgD expression in the spleens of CIA mice in vivo. CIA mice were treated with IgD-Fc-Ig, IgG₁-Fc, rhTNFR:Fc, and anti-mouse IgD antibodies by intravenous administration via the tail. Immunohistochemical analysis of CD40 (a), CD40L (b), and IgD (c) expression in the spleens of CIA mice. Data are expressed as the mean \pm SEM (for each group, five mice). ** $P < 0.01$ vs. normal, # $P < 0.05$ and ## $P < 0.01$ vs. model.

DISCUSSION

Accumulating evidence has indicated the vital role of IgD in RA. Reports focusing on IgDR-related signaling have been limited. Our group found that IgD obviously induced IgDR expression on T cells [11]. CD4⁺ T cells play a vital role in coordinating protective immune responses to various pathogens and contribute to the development of allergies, inflammation, and immune responses in autoimmune diseases [15]. Accumulating evidence suggests that p56 Lck following IgDR crosslinking plays an important role in the activation of downstream events. Lck is an important kinase that mediates T-cell functions by regulating T-cell receptor (TCR) signal transduction, T-cell differentiation and development, and T-cell homeostasis [16]. Here, we observed that IgDR and phosphorylating Lck site (tyr394) were coexpressed on CD4⁺ T cells in healthy controls, and this coexpression could be increased after IgD stimulation. Moreover, we used the Lck inhibitor A770041 to confirm that Lck is the key kinase in signal transduction. Our data showed that IgD upregulated the expression of p-Lck, p-ZAP70, and p-PI3K and induced NF- κ B translocation in an in vitro study. We suggested that IgDR could directly activate the Lck

phosphorylation site (Tyr394), phosphorylate ZAP70 kinase, activate the PI3K downstream signaling pathway, and promote the nuclear translocation of NF- κ B, followed by IgD-IgDR cross-linking. The kinase Lck is recruited to the TCR complex by the colocalization of CD4 or CD8 coreceptor molecules, where Lck can phosphorylate the immunoreceptor tyrosine-based activation motif (ITAM) signaling motif [17]. Each ITAM motif contains two tyrosines, and when phosphorylated, they form a binding site for the tandem SH2 domain of ZAP70 kinase. By binding to phosphorylated ITAM, ZAP70 is recruited to the plasma membrane, and the activation of ZAP70 kinase further stimulates multiple signaling networks downstream, including calcium mobilization and the Ras/MAPK and PI3K pathways [18, 19]. Moreover, ZAP70 plays a critical role in the initiation of T-cell signaling and initiates a sequence of events leading to the activation of the transcription factor NF- κ B, which, in a stepwise procedure, results in the transcription of genes coding for proteins exerting T-cell functions [20, 21]. We hypothesized that the IgD-IgDR-Lck signal transduction mechanism is similar to the TCR signal initiation mode. Our data suggested that IgD could induce

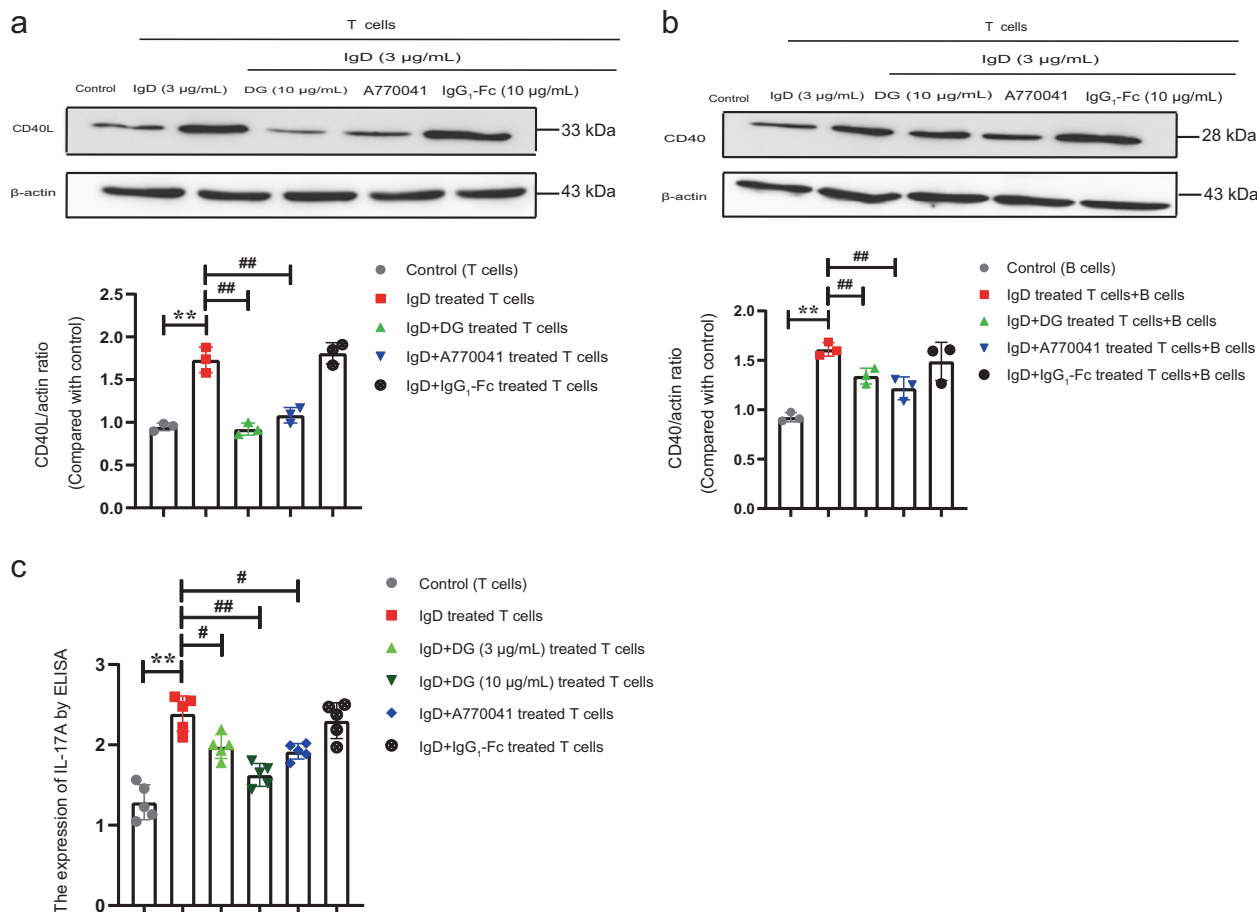


Fig. 7 Effects of IgD-Fc-Ig (DG) on CD4⁺ T-cell and CD19⁺ B-cell actions in CIA mice in vitro. To obtain CD4⁺ T cells and CD19⁺ B cells from the spleens of CIA mice, CD4⁺ T cells were incubated with IgD (3 µg/mL), DG (3, 10 µg/mL), 0.5 µM Lck inhibitor A770041, and IgG₁-Fc (10 µg/mL) in coculture with CD19⁺ B cells in vitro for 48 h. Western blot analysis of CD40L (**a**) and CD40 (**b**) expression on CD4⁺ T cells and CD19⁺ B cells from the spleens of CIA mice. After coculture, CD4⁺ T cells and CD19⁺ B cells were obtained and lysed. **c** ELISA analysis of IL-17A expression in CD4⁺ T-cell supernatant of CIA mice. Data are expressed as the mean ± SEM (both normal group and CIA group 3–5 mice). ***P* < 0.01 vs. control, #*P* < 0.05 and ##*P* < 0.01 vs. IgD (3 µg/mL) stimulation group.

the abnormal activation of T cells by affecting IgDR-Lck-ZAP70-PI3K-NF- κ B signaling and that Lck is a key kinase during the whole process.

The transactivation of CD40L can be tightly regulated by transcription factors such as NF- κ B that bind to the promoter region [22]. Accumulating evidence has demonstrated significant involvement of NF- κ B in the upregulation of CD40L expression in both activated mouse and human T cells [23]. Early CD40L expression was shown to result in B-cell activation, Ig secretion, isotype switching, and memory formation [24]. Compared to healthy controls, CD40L expression is elevated on various cell subsets from patients with SLE, including B cells, T cells, and monocytes [25], as well as on circulating T cells from RA patients [26]. Our previous studies showed that IgD could increase the proportion of CD154⁺ (CD40L) cells in RA patients and CIA mice [9]. In this study, IgD upregulated the expression of CD40L on CD4⁺ T cells and CD40 on CD19⁺ B cells in healthy controls and RA patients. As expected, consistent results were observed in parallel experiments in CIA mice. The engagement of CD40 expressed on the surface of antigen-activated B cells by CD40L expressed on activated CD4⁺ T cells is essential for the initiation and progression of the immune response [27]. Expression of CD40L is dynamically regulated in human CD4⁺ T cells. A few hours after activation, CD4⁺ T cells transiently express CD40L. Later, after the course of proteolytic cleavage, endocytosis, and lysosomal degradation, soluble CD40L is

released as a cytokine [28]. Therefore, we suggest that CD40L is released in a soluble form and acts as a cytokine to interact with B cells in a T–B-cell coculture environment. In addition, the interactions of CD40 and CD40L can induce the costimulatory molecules CD80–CD86, promote the differentiation, proliferation, and maturation of B cells, and promote the excitation and differentiation of T cells [29]. In accordance with this report, we observed that the expression of CD86 on CD19⁺ B cells in RA patients was upregulated after T–B-cell coculture. Our results showed that IgD-activated T cells could induce the activation of B cells by increasing the expression of the costimulatory molecules CD40–CD40L after T–B coculture. In turn, the effect of IgD per se on B-cell activation was not significant. Previous studies shift our focus to IgD–IgDR interactions on T cells, which may offer a potential strategy to neutralize overexpressed IgD in RA.

In recent years, there has been a surge in the development of new biological agents as alternatives to traditional treatment methods for RA, such as the selective T-cell costimulatory modulator abatacept (CTLA-4Ig) and the monoclonal antibody anti-CD20 [30]. Abatacept represents a soluble, recombinant, fully humanized fusion protein comprising the extracellular domain of CTLA-4 and the Fc portion of IgG₁. Abatacept binds to the costimulatory molecules CD80 and CD86 on antigen-presenting cells (APCs), thereby blocking the interaction with CD28 on T cells. In addition, abatacept acts on a wide range of cell populations,

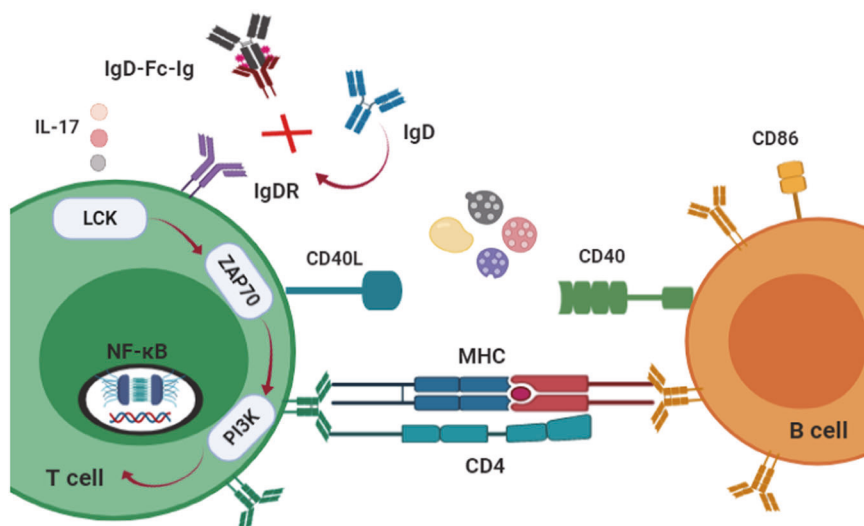


Fig. 8 Hypothetical schematic diagram of the IgD-Fc-Ig mechanism. IgD induces the abnormal activation of T cells by affecting IgDR-Lck-ZAP70-PI3K-NF- κ B signaling in T cells, which can upregulate the expression of CD40L on CD4⁺ T cells. The cocultivation of IgD-activated T cells can upregulate the expression of the costimulatory molecules CD40-CD40L and then promote the activation of B cells. IgD-Fc-Ig downregulated CD86 expression and IL-17A levels and decreased CD40 and CD40L expression. IgD-Fc-Ig restrains the activation of T cells by inhibiting IgD-IgDR-Lck-ZAP70-PI3K-NF- κ B signaling, thus inhibiting the activation of B cells.

including regulatory T cells (Tregs), monocytes/macrophages, osteoclasts, and B cells [31, 32]. Therefore, there is no exact drug target, and its most serious adverse reactions are severe infection and malignant tumors. B-cell lymphoma (including diffuse large B-cell lymphoma) expresses the CD20 marker on the cell surface. Anti-CD20 monoclonal antibody can bind to CD20 on the surface of lymphoma cells, and the other end of the antibody can bind to phagocytes or killer cells. Therefore, lymphoma cells can be engulfed by phagocytes or killed by killer cells. Normal B cells, which play vital roles in the adaptive immune response and express CD20, will also be eliminated [33]. In summary, research on a highly selective and highly targeted therapeutic drug for RA is necessary.

With a particular emphasis on novel T cell-targeted therapeutic strategies, our work highlights the immunologic features of IgD/IgDR and a novel direction for the discovery and development of new drugs for the treatment of T cell-related diseases. Based on these findings, our group successfully linked the human IgD-Fc segment to the human IgG₁-Fc segment to form a fusion protein (IgD-Fc-Ig) targeting IgD/IgDR, and a patent license was acquired in China (No: 201510600762X). Our group confirmed that IgD-Fc-Ig exhibited a similar binding affinity as IgD for IgDR and competitively inhibited IgD binding to IgDR [11]. In a rodent model of CIA, disease activity, manifestation, T-cell activation, and the expression of p-Lck, p-ZAP70, and p-NF- κ B were significantly reduced after IgD-Fc-Ig administration [9, 13]. This study further confirmed that IgD-Fc-Ig could downregulate the interaction of IgDR and p-Lck, downregulate the expression of p-Lck, p-ZAP70, and PI3K, and decrease NF- κ B nuclear translocation followed by IgD stimulation. Then, inhibited T cells restrained B-cell activation by downregulating CD40-CD40L expression. The limitation of this study is that the cell counts of T and B cells in the coculture environment were too limited, and we could hardly detect the cytokines and antibodies secreted from activated T and B cells. Moreover, the IgDR gene has not yet been cloned, and the exact molecular mechanism by which IgD participates in abnormal activation of T and B cells through IgDR is needed. Both in vivo and in vitro experiments verified that IgD-Fc-Ig can competitively block the IgDR-Lck-ZAP70-PI3K signaling pathway, inhibit the abnormal proliferation and activation of T and B cells, and further alleviate RA. IgD-Fc-Ig has the potential to become an

innovative drug for RA treatment with high-level IgD by blocking the IgD-IgDR-Lck signaling pathway.

CONCLUSION

In conclusion, IgD can induce the abnormal activation of T cells by affecting IgDR-Lck-ZAP70-PI3K-NF- κ B signaling in T cells. Coculture of IgD-induced T cells and B cells can upregulate the expression of the costimulatory molecules CD40-CD40L and then promote the activation of B cells. IgD-Fc-Ig restrains the activation of T cells by inhibiting IgD-IgDR-Lck-ZAP70-PI3K-NF- κ B signaling, thus inhibiting the activation of B cells (Fig. 8). These findings provide a theoretical basis for further elucidating the occurrence and development of RA and provide experimental evidence for the development of IgD-Fc-Ig as a new targeted therapeutic drug for highly selective therapy of RA.

ACKNOWLEDGEMENTS

This research was supported by the National Natural Science Foundation of China (Nos. 81603121; 81673444; 81973332) and the Key Projects of Natural Science Research of Anhui Colleges and Universities (No. KJ2020A0158). The authors acknowledge Professors Li Si and Doctor Fang Wang in the First Affiliated Hospital of Anhui Medical University, for their help in healthy and RA donors recruiting.

AUTHOR CONTRIBUTIONS

XXH performed the experiments and wrote the paper. AJZ and WWP participated in the experiments, collected the samples and performed immunohistochemistry experiments. QLX and JYC took part in FACS Aria cell sorting. LLZ and YC helped to revise the paper. YJW designed the study, participated in the experiments, and revised the paper. WW conceived of the study and revised the paper. All authors read and approved the final paper.

ADDITIONAL INFORMATION

Conflict of interest: The authors declare no competing interests.

REFERENCES

- Sparks JA. Rheumatoid arthritis. *Ann Intern Med.* 2019;170:ITC1-16.
- Smolen JS, Landewé RBM, Bijlsma JWJ, Burmester GR, Dougados M, Kerschbaumer A, et al. EULAR recommendations for the management of rheumatoid

- arthritis with synthetic and biological disease-modifying antirheumatic drugs: 2019 update. *Ann Rheum Dis.* 2020;79:685–99.
3. Bécède M, Alasti F, Gessl I, Haupt L, Kerschbaumer A, Landesmann U, et al. Risk profiling for a refractory course of rheumatoid arthritis. *Semin Arthritis Rheum.* 2019;49:211–7.
 4. Preud'homme JL, Petit I, Barra A, Morel F, Lecron JC, Lelièvre E. Structural and functional properties of membrane and secreted IgD. *Mol Immunol.* 2000;37:871–87.
 5. Chen K, Cerutti A. New insights into the enigma of immunoglobulin D. *Immunol Rev.* 2010;237:160–79.
 6. Wu Y, Pan W, Hu X, Zhang A, Wei W. The prospects for targeting FcR as a novel therapeutic strategy in rheumatoid arthritis. *Biochem Pharmacol.* 2021;183:114360.
 7. Chen L, Fan F, Deng J, Xu J, Xu A, Sun C, et al. Clinical characteristics and prognosis of immunoglobulin D myeloma in the novel agent era. *Ann Hematol.* 2019;98:963–70.
 8. Carballo I, Rabuñal N, Alvela L, Pérez LF, Vidal C, Alonso M, et al. Factors influencing serum concentrations of IgD in the adult population: an observational study in Spain. *Scand J Immunol.* 2017;85:272–9.
 9. Zhang J, Hu X, Dong X, Chen W, Wu Y, Wei W, et al. Regulation of T cell activities in rheumatoid arthritis by the novel fusion protein IgD-Fc-Ig. *Front Immunol.* 2020;11:755.
 10. Wu Y, Chen W, Chen H, Zhang L, Huang Q, Wei W, et al. The elevated secreted immunoglobulin D enhanced the activation of peripheral blood mononuclear cells in rheumatoid arthritis. *PLoS ONE.* 2016;11:e147788.
 11. Chen H, Wu Y, Huang Q, Chen W, Dong J, Wei W. Novel fluorescence based ligand-receptor binding assay: study on IgD receptor. *Acta Univ Med Anhui.* 2016;51:1105–10.
 12. Amin AR, Tamma SM, Oppenheim JD, Finkelman FD, Kieda C, Coico RF, et al. Specificity of the murine IgD receptor on T cells is for N-linked glycans on IgD molecules. *Proc Natl Acad Sci USA.* 1991;88:9238–42.
 13. Han L, Zhang XZ, Wang C, Tang X, Zhang L, Wei W, et al. IgD-Fc-Ig fusion protein, a new biological agent, inhibits T cell function in CIA rats by inhibiting IgD-IgDR-Lck-NF- κ B signaling pathways. *Acta Pharmacol Sin.* 2020;41:800–12.
 14. George TC, Fanning SL, Fitzgerald-Bocarsly P, Medeiros RB, High-fill S, Shimizu Y, et al. Quantitative measurement of nuclear translocation events using similarity analysis of multispectral cellular images obtained in flow. *J Immunol Methods.* 2006;311:117–29.
 15. Hu X, Wu Y, Zhang J, Wei W. T-cells interact with B cells, dendritic cells, and fibroblast-like synoviocytes as hub-like key cells in rheumatoid arthritis. *Int Immunopharmacol.* 2019;70:428–34.
 16. Guillaume G, Renaud L, Paul EL. Regulatory mechanisms in T cell receptor signalling. *Nat Rev Immunol.* 2018;18:485–97.
 17. Courtney AH, Lo WL, Weiss A. TCR signaling: mechanisms of initiation and propagation. *Trends Biochem Sci.* 2018;43:108–23.
 18. Simeoni L. Lck activation: puzzling the pieces together. *Oncotarget.* 2017;8:102761–2.
 19. Lo WL, Shah NH, Ahsan N, Horkova V, Stepanek O, Salomon AR, et al. Lck promotes Zap70-dependent LAT phosphorylation by bridging Zap70 to LAT. *Nat Immunol.* 2018;19:733–41.
 20. Ursula B, Burkhardt S, Luca S. Beyond TCR signaling: emerging functions of Lck in cancer and immunotherapy. *Int J Mol Sci.* 2019;20:3500.
 21. Hu J, Luo T, Xi D, Guo K, Hu L, Zhao J, et al. Silencing ZAP70 prevents HSP65-induced reverse cholesterol transport and NF- κ B activation in T cells. *Biomed Pharmacother.* 2018;102:271–7.
 22. Mendez-Samperio P, Ayala H, Vazquez A. NF-kappa B is involved in regulation of CD40 ligand expression on *Mycobacterium bovis* bacillus Calmette-Guerin-activated human T cells. *Clin Diagn Lab Immunol.* 2003;10:376–82.
 23. Ngaoteppuratham T, Kaplan B, Kaminski NE. Impaired NFAT and NF- κ B activation are involved in suppression of CD40 ligand expression by $\Delta(9)$ -tetrahydrocannabinol in human CD4⁺ T cells. *Toxicol Appl Pharmacol.* 2013;273:209–18.
 24. Dakal TC, Dhabhai B, Agarwal D, Gupta R, Nagda G, Meena AR, et al. Mechanistic basis of co-stimulatory CD40-CD40L ligation mediated regulation of immune responses in cancer and autoimmune disorders. *Immunobiology.* 2020;225:151899.
 25. Elmetwali T, Salman A, Wei W, Hussain SA, Young LS, Palmer DH. CD40L membrane retention enhances the immunostimulatory effects of CD40 ligation. *Sci Rep.* 2020;10:342.
 26. Tung CH, Lu MC, Lai NS, Wu SF. Tumor necrosis factor- α blockade treatment decreased CD154 (CD40-ligand) expression in rheumatoid arthritis. *PLoS ONE.* 2017;12:e0183726.
 27. Jodi LK, Sadiye AR, Rachel E, Roland K. Targeting the CD40-CD40L pathway in autoimmune diseases: Humoral immunity and beyond. *Adv Drug Deliv Rev.* 2019;141:92–103.
 28. Elgueta R, Benson MJ, de Vries VC, Wasiuk A, Guo Y, Noelle RJ. Molecular mechanism and function of CD40/CD40L engagement in the immune system. *Immunol Rev.* 2009;229:152–72.
 29. Lorenzetti R, Janowska I, Smulski CR, Frede N, Henneberger N, Walter L, et al. Abatacept modulates CD80 and CD86 expression and memory formation in human B-cells. *J Autoimmun.* 2019;101:145–52.
 30. Abbasi M, Mousavi MJ, Jamalzahi S, Alimohammadi R, Bezvan MH, Mohammadi H, et al. Strategies toward rheumatoid arthritis therapy; the old and the new. *J Cell Physiol.* 2019;234:10018–31.
 31. Bonelli M, Scheinecker C. How does abatacept really work in rheumatoid arthritis? *Curr Opin Rheumatol.* 2018;30:295–300.
 32. Bonelli M, Göschl L, Blüml S, Karonitsch T, Hirahara K, Ferner E, et al. Abatacept (CTLA-4Ig) treatment reduces T cell apoptosis and regulatory T cell suppression in patients with rheumatoid arthritis. *Rheumatology.* 2016;55:710–20.
 33. Du FH, Mills EA, Mao-Draayer Y. Next-generation anti-CD20 monoclonal antibodies in autoimmune disease treatment. *Auto Immun Highlights.* 2017;8:12.